AIAA JOURNAL
Vol. 41, No. 4, April 2003

Effective Coefficients of Piezoelectric Fiber-Reinforced Composites

Nilanjan Mallik* and M. C. Ray†
Indian Institute of Technology, Kharagpur 721 302, India

The effective coefficients of piezoelectric fiber-reinforced composites (PFRC) have been determined through micromechanical analyzes. The method of cells (MOC) and the strength of materials (SM) approach have been employed to predict the coefficients. A constant electric field is considered in the direction transverse to the fiber direction and is assumed to be the same both in the fiber and the matrix. MOC and SM predictions for the effective piezoelectric coefficient of the PFRC assessing the actuating capability in the fiber direction are in excellent agreement. It has been found for the piezoelectric fibers considered that, when the fiber volume fraction exceeds a critical fiber volume fraction, this effective piezoelectric coefficient becomes significantly larger than the corresponding coefficient of the piezoelectric material of the fiber. The methods also show the excellent matching of the predictions of the effective elastic constants and the dielectric constant of the PFRC in the useful range of fiber volume fraction.

Introduction

PIEZOELECTRIC materials exhibit material deformations due to an applied electric field and induce electric charges in response to applied mechanical loads. The use of piezoelectric materials as actuators and sensors is attributed to these two phenomena. When bonded with or embedded in flexible structures, these materials provide the structures with self-monitoring and self-controlling capabilities. A great deal of research has been carried out during the past decade[1–17] to achieve active control of high-performing lightweight flexible structures called "smart structures," using piezoelectric materials as distributed actuators and sensors.

Further efforts toward improving the active damping led to the development of an active constrained layer damping (ACLD) treatment, which combines the attributes of both passive and active damping.[18–20] In ACLD, the active part of the damping is also due to the use of piezoelectric actuator as a constraining layer. Thus, piezoelectric materials are playing a major role in achieving active damping in smart structures. However, the existing monolithic piezoelectric materials being used in smart structures possess low control authority because their piezoelectric stress/strain constants are of small magnitude. Because the active damping of smart structures is dependent on the piezoelectric stress/strain constants, tailoring of these properties may further improve the damping characteristics of lightweight flexible structures.

Currently, piezoelectric composites are being effectively used for underwater transducers and medical imaging applications.[21–23] These composites show improved mechanical performance, electromechanical coupling characteristics, and acoustic impedance matching with the surrounding medium over the piezoelectric material alone. The research on the development of piezoelectric composites is mainly directed toward the micromechanical estimates of their mechanical and electromechanical properties.[24–26] Aboudi[26] carried out a micromechanical analysis to predict the effective coefficients of piezoelectric fiber-reinforced composites, considering different electric fields in the fibers and matrix that are related to average composite electric field. His prediction for the piezoelectric constant, which gives rise to actuation in the fiber direction, does not show any improvement over that of the piezoelectric material alone. Smith and Auld[24] predicted marginal improvement of the effective piezoelectric constant of the piezocomposite that quantifies the deformations in the fiber direction. The constructional features of their composites are that the rods of piezoelectric materials are embedded vertically, that is, aligned along the thickness of the composite, in a polymer base matrix such that the electric fields are applied along the length of the piezoelectric fibers. Such an arrangement of fibers in the composites results in the necessity of tuning the thickness mode of oscillations before using them as transducers. Smith and Auld[24] assumed that the electric fields were the same both in the fibers and in the matrix. To use the piezoelectric composites as the actuators for flexural vibration control of smart structures, the piezoelectric fibers should be oriented longitudinally to render a bending mode of actuations. However, for unidirectional fiber-reinforced composites, it may be practically difficult to apply a constant electric field along the length of the fibers when the fibers are very long and the fibers are aligned with the longitudinal direction. The most practical option is to apply the electric field across the thickness of the composite, that is, in a direction transverse to the fiber direction. Also, because the thickness of the layer of a composite is usually very low, it may not be difficult to maintain a constant electric field across the thickness of the composite. Hence, this paper is concerned with the predictions of the effective elastic and piezoelectric coefficients of unidirectional piezoelectric fiber-reinforced composites (PFRC) subjected to a constant electric field acting in a direction transverse to the fiber direction. The main focus is to determine the effective piezoelectric coefficient of the PFRC that determines the induced normal stress in the fiber direction. Note that this induced stress is a measure of control authority of the actuator made of PFRC. No literature is currently available to compare the predictions. Hence, two methods of micromechanics have been employed to validate the predictions of these effective coefficients.

Effective Properties of Piezoelectric Composites

Figure 1 shows a schematic representation of a lamina made of PFRC. It is assumed that the proposed composite is homogeneous, the fibers are continuous and parallel, and the fiber and matrix materials are linearly elastic. The fibers are subjected to a constant electric field in the direction transverse to the fiber direction, and the electric field is assumed to be the same both in the fibers and in the matrix.[24] In this regard, note that, in the linear constitutive equations of any piezoelectric material, the elastic and piezoelectric coefficients are defined at a constant electric field.[27] This section deals with the procedure of employing two methods of micromechanics, namely, the strength of materials approach (SM) and the method of cells (MOC), to determine the effective piezoelectric coefficients of this lamina.

Received 28 May 2002; revision received 18 October 2002; accepted for publication 18 October 2002.

*Research Scholar, Department of Mechanical Engineering.
†Assistant Professor, Department of Mechanical Engineering; mcray@mech.iitkgp.ernet.in.

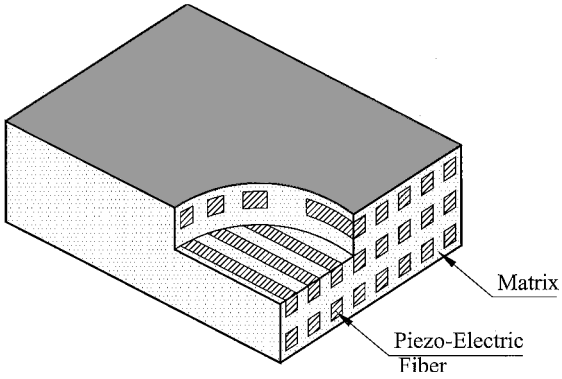

Fig. 1 Schematic diagram of a lamina of PFRC.

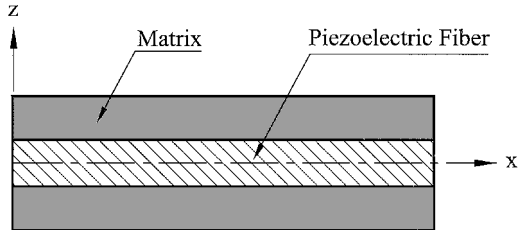

Fig. 2 Longitudinal cross section of a representative volume of PFRC.

SM Approach

In general, the micromechanical analysis is confined to a representative volume (RVE) that includes both fiber and the surrounding matrix. Figure 2 describes the longitudinal cross section of such a representative volume of the lamina shown in Fig. 1. The piezoelectric fibers are oriented longitudinally, that is, along the $\boldsymbol{x}$ axis. The matrix material is a polymer and is piezoelectrically inactive. Although the fibers have been taken to be rectangular in cross section, the actual shape of the fibers does not affect the predictions of the properties effective in the fiber direction. The constitutive relations for the material of the piezoelectric fibers under the action of a transverse electric field only are[27]

$$\sigma_x^p = \boldsymbol{C}_{11}^p \in_x^p + \boldsymbol{C}_{12}^p \in_y^p + \boldsymbol{C}_{13}^p \in_z^p - \boldsymbol{e}_{31}^p \boldsymbol{E}_z \tag{1}$$

$$\sigma_y^p = \boldsymbol{C}_{12}^p \in_x^p + \boldsymbol{C}_{22}^p \in_y^p + \boldsymbol{C}_{23}^p \in_z^p - \boldsymbol{e}_{31}^p \boldsymbol{E}_z \tag{2}$$

$$\sigma_z^p = \boldsymbol{C}_{13}^p \in_x^p + \boldsymbol{C}_{23}^p \in_y^p + \boldsymbol{C}_{33}^p \in_z^p - \boldsymbol{e}_{33}^p \boldsymbol{E}_z \tag{3}$$

$$\sigma_{yz}^p = \boldsymbol{C}_{44}^p \in_{yz}^p \tag{4}$$

$$\sigma_{xz}^p = \boldsymbol{C}_{55}^p \in_{xz}^p \tag{5}$$

$$\sigma_{xy}^p = \boldsymbol{C}_{66}^p \in_{xy}^p \tag{6}$$

$$\boldsymbol{D}_z^p = \boldsymbol{e}_{31}^p \in_x^p + \boldsymbol{e}_{31}^p \in_y^p + \boldsymbol{e}_{33}^p \in_z^p + \varepsilon_{33}^p \boldsymbol{E}_z \tag{7}$$

and those for the matrix material are

$$\sigma_x^m = \boldsymbol{C}_{11}^m \in_x^m + \boldsymbol{C}_{12}^m \in_y^m + \boldsymbol{C}_{13}^m \in_z^m \tag{8}$$

$$\sigma_y^m = \boldsymbol{C}_{12}^m \in_x^m + \boldsymbol{C}_{22}^m \in_y^m + \boldsymbol{C}_{23}^m \in_z^m \tag{9}$$

$$\sigma_z^m = \boldsymbol{C}_{13}^m \in_x^m + \boldsymbol{C}_{23}^m \in_y^m + \boldsymbol{C}_{33}^m \in_z^m \tag{10}$$

$$\sigma_{yz}^m = \boldsymbol{C}_{44}^m \in_{yz}^m \tag{11}$$

$$\boldsymbol{\sigma}_{xz}^m = \boldsymbol{C}_{55}^m \in_{xz}^m \tag{12}$$

$$\sigma_{xy}^m = \boldsymbol{C}_{66}^m \in_{xy}^m \tag{13}$$

$$\boldsymbol{D}_z^m = \varepsilon_{33}^m \boldsymbol{E}_z \tag{14}$$

in which, σ_x, σ_y, and σ_z are the normal stresses in the $\boldsymbol{x}$, $\boldsymbol{y}$, and $\boldsymbol{z}$ directions, respectively; σ_{xz} and σ_{yz} are the transverse shear stresses; σ_{xy} is the in-plane shear stress; $\in_x$, $\in_y$, $\in_z$, $\in_{xz}$, $\in_{yz}$, and $\in_{xy}$ are the corresponding strains; $\boldsymbol{C}_{ij}$, $\boldsymbol{i}$, $\boldsymbol{j} = 1, 2, 3$, are the elastic constants; $\boldsymbol{e}_{31}$ and $\boldsymbol{e}_{33}$ are the piezoelectric stress constants; ε_{33} is the dielectric constant; $\boldsymbol{D}_z$ is the electric displacement in the $\boldsymbol{z}$ direction; and $\boldsymbol{E}_z$ is the electric field applied across the thickness of the lamina, that is, along the $\boldsymbol{z}$ direction. The superscripts p and m denote the fiber and matrix, respectively. Note that the piezoelectric constants $\boldsymbol{e}_{31}$ and $\boldsymbol{e}_{33}$ are the measure of induced normal stresses in the $\boldsymbol{x}$ and $\boldsymbol{z}$ directions, respectively, due to the applied unit electric field in the $\boldsymbol{z}$ direction. The objective of this section is to determine the corresponding piezoelectric constants of the overall composites. It is assumed that no slippage occurs at the fiber–matrix interface during the longitudinal mode of deformation. This implies the existence of perfect bonding between the fiber and matrix. Thus, the normal strains in the $\boldsymbol{x}$ direction are the same in both phases and are equal to the composite strain $\in_x^c$, that is,

$$\in_x^p = \in_x^m = \in_x^c \tag{15}$$

Also, it is assumed that the lateral stresses in the $\boldsymbol{y}$ and $\boldsymbol{z}$ directions are the same in both phases and are equal to the respective composite stresses, σ_y^c and σ_z^c, that is,

$$\sigma_y^p = \sigma_y^m = \sigma_y^c \tag{16}$$

$$\sigma_z^p = \sigma_z^m = \sigma_z^c \tag{17}$$

By the use of the rule of mixture, the normal strains $\in_y^c$ and $\in_z^c$ in the PFRC in the $\boldsymbol{y}$ and $\boldsymbol{z}$ directions, respectively, can be written as

$$\in_y^c = \boldsymbol{v}_f \in_y^p + (1 - \boldsymbol{v}_f) \in_y^m \tag{18}$$

$$\in_z^c = \boldsymbol{v}_f \in_z^p + (1 - \boldsymbol{v}_f) \in_z^m \tag{19}$$

where $\boldsymbol{v}_f$ is the fiber volume fraction. By the use of the relations (2), (3), (9), (10), and (15–19), the normal strains $\in_y^p$ and $\in_z^p$ can be written in terms of the composite normal strains $\in_x^c$, $\in_y^c$, and $\in_z^c$ and the electric field $\boldsymbol{E}_z$, as follows:

$$\in_y^p = (1/\boldsymbol{L})\left(\boldsymbol{c}_1 \in_x^c - \boldsymbol{c}_2 \in_y^c - \boldsymbol{c}_3 \in_z^c - \boldsymbol{c}_4 \boldsymbol{E}_z\right) \tag{20}$$

$$\in_z^p = (1/\boldsymbol{L})\left(-\boldsymbol{c}_5 \in_x^c + \boldsymbol{c}_6 \in_y^c + \boldsymbol{c}_7 \in_z^c + \boldsymbol{c}_8 \boldsymbol{E}_z\right) \tag{21}$$

where

$$\boldsymbol{L} = \left(\boldsymbol{v}_m \boldsymbol{C}_{22}^p + \boldsymbol{v}_f \boldsymbol{C}_{22}^m\right)\left(\boldsymbol{v}_m \boldsymbol{C}_{33}^p + \boldsymbol{v}_f \boldsymbol{C}_{33}^m\right) - \left(\boldsymbol{v}_m \boldsymbol{C}_{23}^p + \boldsymbol{v}_f \boldsymbol{C}_{23}^m\right)^2$$

$$\boldsymbol{c}_1 = \boldsymbol{v}_m\left[\left(\boldsymbol{C}_{13}^p - \boldsymbol{C}_{13}^m\right)\left(\boldsymbol{v}_m \boldsymbol{C}_{23}^p + \boldsymbol{v}_f \boldsymbol{C}_{23}^m\right) - \left(\boldsymbol{C}_{12}^p - \boldsymbol{C}_{12}^m\right)\left(\boldsymbol{v}_m \boldsymbol{C}_{33}^p + \boldsymbol{v}_f \boldsymbol{C}_{33}^m\right)\right]$$

$$\boldsymbol{c}_2 = \boldsymbol{C}_{23}^m\left(\boldsymbol{v}_m \boldsymbol{C}_{23}^p + \boldsymbol{v}_f \boldsymbol{C}_{23}^m\right) - \boldsymbol{C}_{22}^m\left(\boldsymbol{v}_m \boldsymbol{C}_{33}^p + \boldsymbol{v}_f \boldsymbol{C}_{33}^m\right)$$

$$\boldsymbol{c}_3 = \boldsymbol{C}_{33}^m\left(\boldsymbol{v}_m \boldsymbol{C}_{23}^p + \boldsymbol{v}_f \boldsymbol{C}_{23}^m\right) - \boldsymbol{C}_{23}^m\left(\boldsymbol{v}_m \boldsymbol{C}_{33}^p + \boldsymbol{v}_f \boldsymbol{C}_{33}^m\right)$$

$$\boldsymbol{c}_4 = \boldsymbol{v}_m\left[\boldsymbol{e}_{33}^p\left(\boldsymbol{v}_m \boldsymbol{C}_{23}^p + \boldsymbol{v}_f \boldsymbol{C}_{23}^m\right) - \boldsymbol{e}_{31}^p\left(\boldsymbol{v}_m \boldsymbol{C}_{33}^p + \boldsymbol{v}_f \boldsymbol{C}_{33}^m\right)\right]$$

$$\boldsymbol{c}_5 = \boldsymbol{v}_m\left[\left(\boldsymbol{C}_{13}^p - \boldsymbol{C}_{13}^m\right)\left(\boldsymbol{v}_m \boldsymbol{C}_{22}^p + \boldsymbol{v}_f \boldsymbol{C}_{22}^m\right) - \left(\boldsymbol{C}_{12}^p - \boldsymbol{C}_{12}^m\right)\left(\boldsymbol{v}_m \boldsymbol{C}_{23}^p + \boldsymbol{v}_f \boldsymbol{C}_{23}^m\right)\right]$$

$$\boldsymbol{c}_6 = \boldsymbol{C}_{23}^m\left(\boldsymbol{v}_m \boldsymbol{C}_{22}^p + \boldsymbol{v}_f \boldsymbol{C}_{22}^m\right) - \boldsymbol{C}_{22}^m\left(\boldsymbol{v}_m \boldsymbol{C}_{23}^p + \boldsymbol{v}_f \boldsymbol{C}_{23}^m\right)$$

$$\boldsymbol{c}_7 = \boldsymbol{C}_{33}^m\left(\boldsymbol{v}_m \boldsymbol{C}_{22}^p + \boldsymbol{v}_f \boldsymbol{C}_{22}^m\right) - \boldsymbol{C}_{23}^m\left(\boldsymbol{v}_m \boldsymbol{C}_{23}^p + \boldsymbol{v}_f \boldsymbol{C}_{23}^m\right)$$

$$\boldsymbol{c}_8 = \boldsymbol{v}_m\left[\boldsymbol{e}_{33}^p\left(\boldsymbol{v}_m \boldsymbol{C}_{22}^p + \boldsymbol{v}_f \boldsymbol{C}_{22}^m\right) - \boldsymbol{e}_{31}^p\left(\boldsymbol{v}_m \boldsymbol{C}_{23}^p + \boldsymbol{v}_f \boldsymbol{C}_{23}^m\right)\right]$$

Axial force equilibrium of the composite requires that the composite stress σ_x^c in the $\boldsymbol{x}$ direction can be written using the rule of mixture as

$$\sigma_x^c = \boldsymbol{v}_f \sigma_x^p + (1 - \boldsymbol{v}_f)\sigma_x^m \tag{22}$$

Substitution of Eqs. (1) and (8) into Eq. (22), in conjunction with the use of relations (18–21), yields the final expression for σ_x^c, as follows:

$$\sigma_x^c = \boldsymbol{C}_{11}^c \in_x^c + \boldsymbol{C}_{12}^c \in_y^c + \boldsymbol{C}_{13}^c \in_z^c - \boldsymbol{e}_{31}^c \boldsymbol{E}_z \tag{23}$$

in which $\boldsymbol{C}_{11}^c$, $\boldsymbol{C}_{12}^c$, and $\boldsymbol{C}_{13}^c$ are the effective elastic coefficients of the PFRC and $\boldsymbol{e}_{31}^c$ is the effective piezoelectric coefficient of the PFRC that quantifies the induced normal stress in the longitudinal $\boldsymbol{x}$ direction due to the unit electric field acting in the $\boldsymbol{z}$ direction. The expressions for $\boldsymbol{C}_{11}^c$, $\boldsymbol{C}_{12}^c$, and $\boldsymbol{C}_{13}^c$ are not shown here. However, they can be easily identified while deriving Eq. (23). The expression for $\boldsymbol{e}_{31}^c$ is obtained as follows:

$$\begin{aligned}\boldsymbol{e}_{31}^c = {} & \boldsymbol{v}_f \boldsymbol{e}_{31}^p - (\boldsymbol{v}_m \boldsymbol{v}_f / \boldsymbol{L})\Big\{\big(\boldsymbol{C}_{13}^p - \boldsymbol{C}_{13}^m\big)\Big[\big(\boldsymbol{v}_m \boldsymbol{C}_{22}^p + \boldsymbol{v}_f \boldsymbol{C}_{22}^m\big)\boldsymbol{e}_{33}^p \\ & - \big(\boldsymbol{v}_m \boldsymbol{C}_{23}^p + \boldsymbol{v}_f \boldsymbol{C}_{23}^m\big)\boldsymbol{e}_{31}^p\Big] + \big(\boldsymbol{C}_{12}^p - \boldsymbol{C}_{12}^m\big)\Big[\big(\boldsymbol{v}_m \boldsymbol{C}_{33}^p + \boldsymbol{v}_f \boldsymbol{C}_{33}^m\big)e_{31}^p \\ & - \big(\boldsymbol{v}_m \boldsymbol{C}_{23}^p + \boldsymbol{v}_f \boldsymbol{C}_{23}^m\big)\boldsymbol{e}_{33}^p\Big]\Big\}\end{aligned} \tag{24}$$

In a similar manner, when Eqs. (2) and (3) and (16–21) are used, the other effective piezoelectric coefficients $\boldsymbol{e}_{32}^c$ and $\boldsymbol{e}_{33}^c$, which quantify the induced normal stresses in the $\boldsymbol{y}$ and $\boldsymbol{z}$ directions, respectively, due to the applied unit electric field in the $\boldsymbol{z}$ direction are obtained as follows:

$$\begin{aligned}\boldsymbol{e}_{32}^c = {} & \boldsymbol{e}_{31}^p + (\boldsymbol{v}_m / L)\Big\{\boldsymbol{C}_{22}^p\Big[\big(\boldsymbol{v}_m \boldsymbol{C}_{23}^p + \boldsymbol{v}_f \boldsymbol{C}_{23}^m\big)\boldsymbol{e}_{33}^p \\ & - \big(\boldsymbol{v}_m \boldsymbol{C}_{33}^p + \boldsymbol{v}_f \boldsymbol{C}_{33}^m\big)\boldsymbol{e}_{31}^p\Big] - \boldsymbol{C}_{23}^p\Big[\big(\boldsymbol{v}_m \boldsymbol{C}_{22}^p + \boldsymbol{v}_f \boldsymbol{C}_{22}^m\big)\boldsymbol{e}_{33}^p \\ & - \big(\boldsymbol{v}_m \boldsymbol{C}_{23}^p + \boldsymbol{v}_f \boldsymbol{C}_{23}^m\big)\boldsymbol{e}_{31}^p\Big]\Big\}\end{aligned} \tag{25}$$

$$\begin{aligned}\boldsymbol{e}_{33}^c = {} & \boldsymbol{e}_{33}^p + (\boldsymbol{v}_m / L)\Big\{\boldsymbol{C}_{23}^p\Big[\big(\boldsymbol{v}_m \boldsymbol{C}_{23}^p + \boldsymbol{v}_f \boldsymbol{C}_{23}^m\big)\boldsymbol{e}_{33}^p \\ & - \big(\boldsymbol{v}_m \boldsymbol{C}_{33}^p + \boldsymbol{v}_f \boldsymbol{C}_{33}^m\big)\boldsymbol{e}_{31}^p\Big] - \boldsymbol{C}_{33}^p\Big[\big(\boldsymbol{v}_m \boldsymbol{C}_{22}^p + \boldsymbol{v}_f \boldsymbol{C}_{22}^m\big)\boldsymbol{e}_{33}^p \\ & - \big(\boldsymbol{v}_m \boldsymbol{C}_{23}^p + \boldsymbol{v}_f \boldsymbol{C}_{23}^m\big)\boldsymbol{e}_{31}^p\Big]\Big\}\end{aligned} \tag{26}$$

MOC

To employ the MOC, the RVE is subdivided into an $\boldsymbol{MN}$ number of rectangular parallelepiped subcells, with $\boldsymbol{M}$ and $\boldsymbol{N}$ being the number of subdivisions along the width and height of the RVE, respectively. Figure 3 illustrates the transverse cross section of such an RVE. The volume of each subcell is

$$\boldsymbol{V}_{\alpha\beta} = \ell \boldsymbol{b}_\alpha \boldsymbol{h}_\beta \tag{27}$$

where the indices α and β identify the location of the subcell in the RVE in the $\boldsymbol{y}$ and $\boldsymbol{z}$ directions, respectively, and $\boldsymbol{b}_\alpha$, $\boldsymbol{h}_\beta$, and ℓ are the width, height, and length of the subcell, respectively. The volume of the RVE is

$$\boldsymbol{V} = \ell \boldsymbol{b} \boldsymbol{h} \tag{28}$$

with

$$\boldsymbol{b} = \sum_{\alpha=1}^{M} \boldsymbol{b}_\alpha, \qquad \boldsymbol{h} = \sum_{\beta=1}^{N} \boldsymbol{h}_\beta$$

The constitutive equations for the medium of a subcell are given either by Eqs. (1–7) or by Eqs. (8–14), depending on whether the medium is a fiber or matrix. These equations can be expressed in a compact form as

$$\{\boldsymbol{X}\}_{\alpha\beta} = [\boldsymbol{Z}]_{\alpha\beta}\{\boldsymbol{Y}\}_{\alpha\beta} \tag{29}$$

in which

$$\{\boldsymbol{X}\}_{\alpha\beta} = \Big[\sigma_x^{\alpha\beta} \quad \sigma_y^{\alpha\beta} \quad \sigma_z^{\alpha\beta} \quad \sigma_{xy}^{\alpha\beta} \quad \sigma_{yz}^{\alpha\beta} \quad \sigma_{xz}^{\alpha\beta} \quad \boldsymbol{D}_z^{\alpha\beta}\Big]^T$$

$$\{\boldsymbol{Y}\}_{\alpha\beta} = \Big[\in_x^{\alpha\beta} \quad \in_y^{\alpha\beta} \quad \in_z^{\alpha\beta} \quad \in_{xy}^{\alpha\beta} \quad \in_{yz}^{\alpha\beta} \quad \in_{xz}^{\alpha\beta} \quad \boldsymbol{E}_z^{\alpha\beta}\Big]^T$$

$$[\boldsymbol{Z}]_{\alpha\beta} = \begin{bmatrix} [\boldsymbol{C}]^{\alpha\beta} & -[\boldsymbol{e}] \\ [\boldsymbol{e}]^T & \varepsilon_{33}^{\alpha\beta} \end{bmatrix}, \qquad [\boldsymbol{e}]^T = \Big[\boldsymbol{e}_{31}^{\alpha\beta} \quad \boldsymbol{e}_{32}^{\alpha\beta} \quad \boldsymbol{e}_{33}^{\alpha\beta} \quad 0 \quad 0 \quad 0\Big]$$

and $[\boldsymbol{C}]$ is the matrix of elastic constants of the material of the subcell. Note that, although the superscript $\alpha\beta$ of the elements in $\{\boldsymbol{X}\}_{\alpha\beta}$, $\{\boldsymbol{Y}\}_{\alpha\beta}$, $[\boldsymbol{Z}]_{\alpha\beta}$, and elsewhere indicate the subcell location, p and m are to be used for $\alpha\beta$ according as the medium of the subcell under consideration is a fiber or matrix, respectively, while $[\boldsymbol{Z}]_{\alpha\beta}$ and $[\boldsymbol{e}]$ are evaluated. Also, in the case of matrix material, $[\boldsymbol{e}]$ will be a null vector.

In micromechanics, the effective properties are determined by evaluating the properties of the repeating cells filled up with the equivalent homogeneous materials. This amounts to volume averaging of the quantity concerned. Thus, the volume average of the strains and electric field in an RVE can be considered as the strains and electric field of the composite. Consequently, the vector $\{\boldsymbol{Y}\}$ containing the composite strains and electric field can be written as

$$\{\boldsymbol{Y}\} = \frac{1}{\boldsymbol{V}} \sum_{\alpha=1}^{M} \sum_{\beta=1}^{N} \boldsymbol{V}_{\alpha\beta}\{\boldsymbol{Y}\}_{\alpha\beta} \tag{30}$$

Similarly, averaging the vectors $\{\boldsymbol{X}\}_{\alpha\beta}$ over the volume of the RVE results in the vector $\{\boldsymbol{X}\}$, containing the stresses and electric displacement for the composite, as follows:

$$\{\boldsymbol{X}\} = \frac{1}{\boldsymbol{V}} \sum_{\alpha=1}^{M} \sum_{\beta=1}^{N} \boldsymbol{V}_{\alpha\beta}\{\boldsymbol{X}\}_{\alpha\beta} \tag{31}$$

It is obvious that the matrix relating the vectors $\{\boldsymbol{X}\}$ and $\{\boldsymbol{Y}\}$ yields the effective properties of PFRC. As in the case of the SM approach, the longitudinal strains in each subcell can be assumed to be the same and equal to that of the composite. This implies perfect bonding between the fiber phase and the matrix phase and leads to the following $\boldsymbol{MN}$ number of equations:

$$\in_x^{\alpha\beta} = \in_x, \qquad \alpha = 1, 2, \ldots, \boldsymbol{M}, \qquad \beta = 1, 2, \ldots, \boldsymbol{N} \tag{32}$$

Also, for perfectly bonded materials, satisfaction of the conditions for continuity of displacements along the subcell interfaces, as well as along the interfaces between the representative volume elements, yields the following $2(\boldsymbol{M}+\boldsymbol{N})+1$ number of equations[26]:

$$\sum_{\alpha=1}^{M} \boldsymbol{b}_\alpha \in_y^{\alpha\beta} = \boldsymbol{b} \in_y, \qquad \beta = 1, 2, \ldots, \boldsymbol{N} \tag{33}$$

$$\sum_{\beta=1}^{N} \boldsymbol{h}_\beta \in_z^{\alpha\beta} = \boldsymbol{h} \in_z, \qquad \alpha = 1, 2, \ldots, \boldsymbol{M} \tag{34}$$

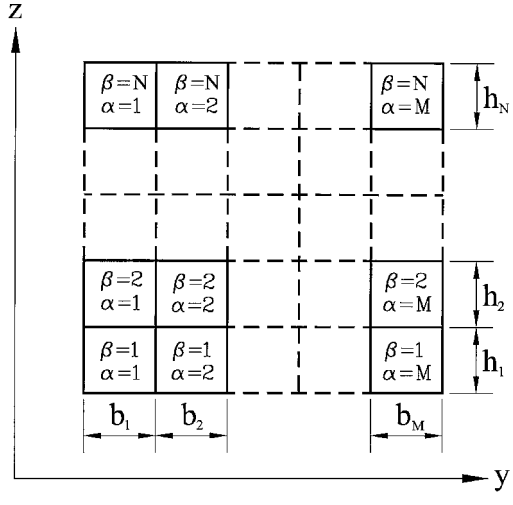

Fig. 3 Transverse cross section of a representative volume consisting of the subcells.

$$\sum_{\alpha=1}^{M}\sum_{\beta=1}^{N} \boldsymbol{b}_\alpha \boldsymbol{h}_\beta \in_{yz}^{\alpha\beta} = \boldsymbol{bh} \in_{yz} \tag{35}$$

$$\sum_{\beta=1}^{N} \ell \boldsymbol{h}_\beta \in_{xz}^{\alpha\beta} = \ell \boldsymbol{h} \in_{xz}, \qquad \alpha = 1, 2, \ldots, \boldsymbol{M} \tag{36}$$

$$\sum_{\alpha=1}^{M} \ell \boldsymbol{b}_\alpha \in_{xy}^{\alpha\beta} = \ell \boldsymbol{b} \in_{xy}, \qquad \beta = 1, 2, \ldots, \boldsymbol{N} \tag{37}$$

Because the electric field is constant along the z direction and is assumed to be the same in both the fiber and matrix, the relation between the electric field in subcells and that in cells leads to another set of an $\boldsymbol{MN}$ number of equations, as follows:

$$\boldsymbol{E}_z^{\alpha\beta} = \boldsymbol{E}_z, \qquad \alpha = 1, 2, \ldots, \boldsymbol{M}, \qquad \beta = 1, 2, \ldots, \boldsymbol{N} \tag{38}$$

The continuity conditions for stresses at the interface between two subcells, as well as between the neighboring RVE, must be maintained. They provide the following $5\boldsymbol{MN} - 2(\boldsymbol{M}+\boldsymbol{N}) - 1$ number of equations[26]:

$$\sigma_y^{\alpha\beta} = \sigma_y^{(\alpha+1)\beta}, \qquad \alpha = 1, 2, \ldots, \boldsymbol{M}-1, \qquad \beta = 1, 2, \ldots, \boldsymbol{N} \tag{39}$$

$$\sigma_z^{\alpha\beta} = \sigma_z^{\alpha(\beta+1)}, \qquad \alpha = 1, 2, \ldots, \boldsymbol{M}, \qquad \beta = 1, 2, \ldots, \boldsymbol{N}-1 \tag{40}$$

$$\sigma_{yz}^{\alpha\beta} = \sigma_{yz}^{(\alpha+1)\beta}, \qquad \alpha = 1, 2, \ldots, \boldsymbol{M}-1, \qquad \beta = 1, 2, \ldots, \boldsymbol{N} \tag{41}$$

$$\sigma_{zx}^{\alpha\beta} = \sigma_{zx}^{\alpha(\beta+1)}, \qquad \alpha = 1, 2, \ldots, \boldsymbol{M}, \qquad \beta = 1, 2, \ldots, \boldsymbol{N}-1 \tag{42}$$

$$\sigma_{yx}^{\alpha\beta} = \sigma_{yx}^{(\alpha+1)\beta}, \qquad \alpha = 1, 2, \ldots, \boldsymbol{M}-1, \qquad \beta = 1, 2, \ldots, \boldsymbol{N} \tag{43}$$

$$\sigma_{zy}^{\alpha\beta} = \sigma_{zy}^{\alpha(\beta+1)}, \qquad \alpha = \boldsymbol{M}, \qquad \beta = 1, 2, \ldots, \boldsymbol{N}-1 \tag{44}$$

With the constitutive relations for the fiber and matrix, the total $7\boldsymbol{MN}$ number of equations given by Eqs. (32–44), can be arranged in a matrix form, as follows:

$$[\boldsymbol{A}]\{\boldsymbol{Y}\}_s = [\boldsymbol{B}]\{\boldsymbol{Y}\} \tag{45}$$

in which $\{\boldsymbol{Y}\}_s$ and $\{\boldsymbol{Y}\}$ are the vectors of subcell quantities taken together and of the composite quantities, respectively. $[\boldsymbol{A}]$ and $[\boldsymbol{B}]$ are the matrices containing the coefficients of subcells and composite quantities, respectively. Note that $\{\boldsymbol{Y}\}_s$ is a vector containing a $7\boldsymbol{MN}$ number of subcell quantities. Thus, the matrix $[\boldsymbol{A}]$ turns out to be a square matrix, and the subcell quantities can be expressed in terms of corresponding composite quantities, as follows:

$$\{\boldsymbol{Y}\}_s = [\boldsymbol{A}]_c\{\boldsymbol{Y}\} \tag{46}$$

in which $[\boldsymbol{A}]_c = [\boldsymbol{A}]^{-1}[\boldsymbol{B}]$. The matrix $[\boldsymbol{A}]_c$ can be treated as an electromechanical concentration matrix. Partitioning $[\boldsymbol{A}]_c$, one can obtain the electromechanical concentration matrix for each subcell $[\boldsymbol{A}]_c^{\alpha\beta}$. When this concentration matrix and Eq. (29) are used, the following can be written:

$$\{\boldsymbol{Y}\}_{\alpha\beta} = [\boldsymbol{A}]_c^{\alpha\beta}\{\boldsymbol{Y}\} \tag{47}$$

$$\{\boldsymbol{X}\}_{\alpha\beta} = [\boldsymbol{Z}]_{\alpha\beta}[\boldsymbol{A}]_c^{\alpha\beta}\{\boldsymbol{Y}\} \tag{48}$$

Finally, using Eq. (48) in Eq. (31), the constitutive relations for the PFRC proposed in this study can be obtained, as follows:

$$\{\boldsymbol{X}\} = [\boldsymbol{Z}]\{\boldsymbol{Y}\} \tag{49}$$

in which

$$[\boldsymbol{Z}] = \frac{1}{\boldsymbol{V}}\sum_{\alpha=1}^{M}\sum_{\beta=1}^{N} \boldsymbol{V}_{\alpha\beta}[\boldsymbol{Z}]_{\alpha\beta}[\boldsymbol{A}]_c^{\alpha\beta} \tag{50}$$

The matrix $[\boldsymbol{Z}]$ contains the effective elastic and piezoelectric properties of the PFRC considered here.

Results and Discussion

The numerical values of the effective properties of the PFRC are evaluated using the two methods of micromechanics discussed in the preceding section. Three different composites of the same matrix material have been considered for numerical results, and the values of $\boldsymbol{M}$ and $\boldsymbol{N}$ are taken as two. The elastic and electric properties of the fibers and matrix of the composites are given in Table 1. The following nondimensional parameters are used to compare the effective piezoelectric coefficients of the PFRC with the corresponding coefficients of the piezoelectric materials of the fibers:

$$\boldsymbol{R}_{31} = \boldsymbol{e}_{31}^c \big/ \boldsymbol{e}_{31}^p, \qquad \boldsymbol{R}_{32} = \boldsymbol{e}_{32}^c \big/ \boldsymbol{e}_{31}^p, \qquad \boldsymbol{R}_{33} = \boldsymbol{e}_{33}^c \big/ \boldsymbol{e}_{33}^p \tag{51}$$

Figure 4 illustrates the variations of the ratio $\boldsymbol{R}_{31}$ between the effective piezoelectric constant $\boldsymbol{e}_{31}^c$ and the piezoelectric constant of the fiber $\boldsymbol{e}_{31}^p$ with the fiber volume fraction. Displayed in Fig. 4 are the predictions obtained by both the SM approach and the MOC for a PZT5/polymer composite. Note that the predictions by both methods are in excellent agreement in the useful range of fiber volume fractions (0.3–0.7) and differ marginally when the fiber volume fraction is in the range of 0.8–0.95. Figures 5 and 6 also illustrate the similar predictions for PZT7A/polymer and PZT5H/polymer composites, respectively. Note from Figs. 4–6 that, for the combinations of the piezoelectric fiber and the polymer matrix considered in this study, if the fiber volume fraction exceeds a critical fiber volume fraction, the value of $\boldsymbol{e}_{31}^c$ becomes greater than the corresponding constant of the piezoelectric fiber alone ($\boldsymbol{R}_{31} > 1$). Because both methods predict almost identical results for $\boldsymbol{e}_{31}^c$, it may be concluded that this effective constant can be authentically used to model the PFRC as distributed actuators.

Table 1 shows that each fiber material is characterized by the magnitude of a ratio $|\boldsymbol{e}_{33}^p/\boldsymbol{e}_{31}^p|$. For a given fiber volume fraction $\boldsymbol{V}_f$,

Table 1 Material properties of fibers and matrix

Fiber/ matrix	$\boldsymbol{C}_{11}$, GPa	$\boldsymbol{C}_{12}$, GPa	$\boldsymbol{C}_{13}$, GPa	$\boldsymbol{C}_{33}$, GPa	$\boldsymbol{e}_{31}$, C/m^2	$\boldsymbol{e}_{33}$, C/m^2	$\lvert\boldsymbol{e}_{33}/\boldsymbol{e}_{31}\rvert$	ε_{33}, C/Vm
PZT-5	121	75.4	75.2	111	−5.4	15.8	2.93	7.35×10^{-9}
PZT-7A	148	76.2	74.2	131	−2.1	9.5	4.54	2.07×10^{-9}
PZT-5H	151	98	96	124	−5.1	27	5.3	13.27×10^{-9}
Epoxy	3.86	2.57	2.57	3.86	0	0	0	0.079×10^{-9}

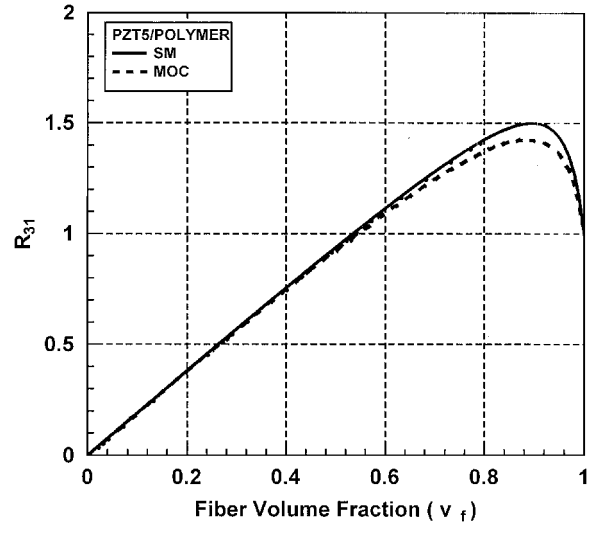

Fig. 4 Variation of the effective piezoelectric coefficient $\boldsymbol{e}_{31}^c$ of PZT5/polymer composite with the fiber volume fraction.

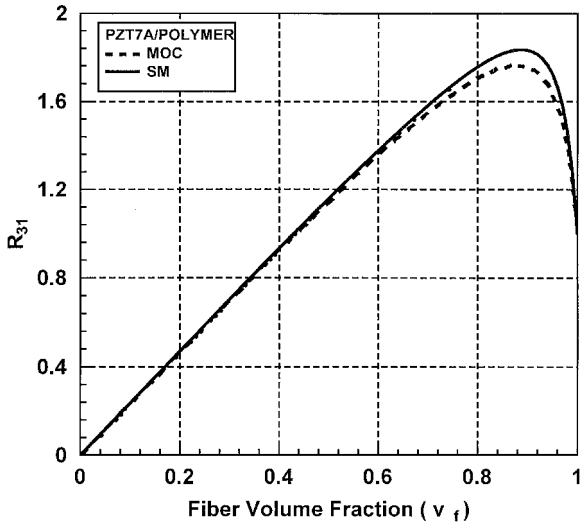

Fig. 5 Variation of the effective piezoelectric coefficient e_{31}^c of PZT7A/polymer composite with the fiber volume fraction.

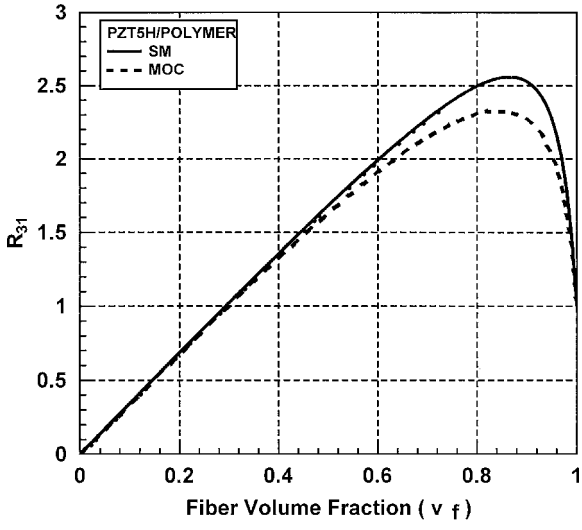

Fig. 6 Variation of the effective piezoelectric coefficient e_{31}^c of PZT5H/polymer composite with the fiber volume fraction.

an expression for e_{31}^c/e_{31}^p can be derived from Eq. (24) as a linear function of $|e_{33}^p/e_{31}^p|$. For the constituent materials of the PFRC considered here, note that the slope of the function is positive. Hence, for a particular fiber volume fraction, the magnitude of the effective piezoelectric coefficient e_{31}^c increases with the increase in the magnitude of the ratio $|e_{33}^p/e_{31}^p|$, as shown in Fig. 7. The predictions of the other effective piezoelectric constants e_{32}^c and e_{33}^c of the PFRC, inducing normal stresses in the y and z directions, respectively, have been presented in Figs. 8 and 9 for PZT5H/polymer composite. The MOC overpredicts the values of these constants as compared to SM approach. Similar results are also obtained for two other composites that are not shown here. The difference between the results for e_{32}^c by both methods can be attributed to the fact that, while deriving the effective properties by the MOC, averaging is performed to obtain the matrix $[Z]$ as given by Eq. (50), from which the results for the corresponding effective property have been extracted. Equations (22) and (23) also imply that averaging is employed in the SM approach to derive the expression for σ_x^c, leading to the derivation of the expression for e_{31}^c given by Eq. (24). The prediction of e_{31}^c shows excellent agreement with that by the MOC. However, the derivation of the expression for σ_y^c by the SM approach does not require averaging, and, hence, the prediction of e_{32}^c by the SM approach differs from that by the MOC. However, note that the effective piezoelectric constant e_{32}^c is not as important as e_{31}^c because the actuation in the fiber direction is the main concern for developing such piezocomposites.

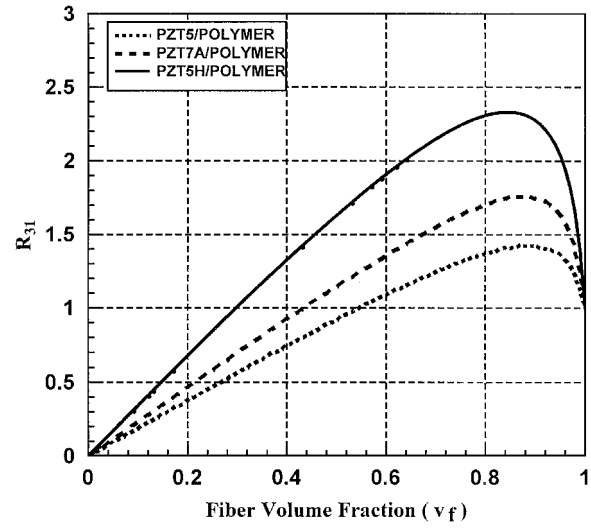

Fig. 7 Influence of the magnitude of e_{33}^p/e_{31}^p on the effective piezoelectric coefficient e_{31}^c of the PFRC.

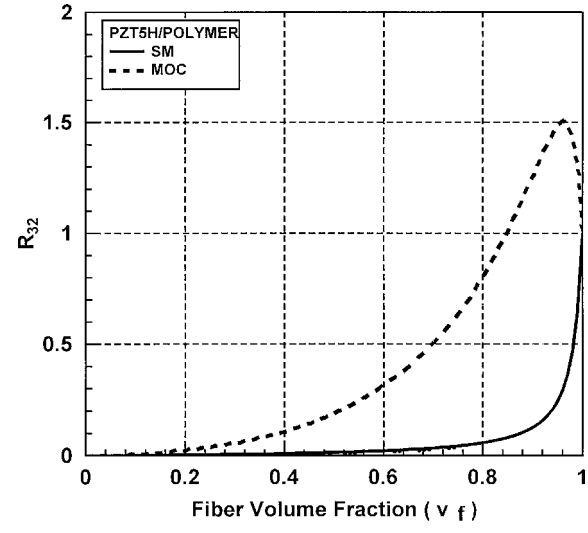

Fig. 8 Variation of the effective piezoelectric coefficient e_{32}^c of PZT5H/polymer composite with the fiber volume fraction.

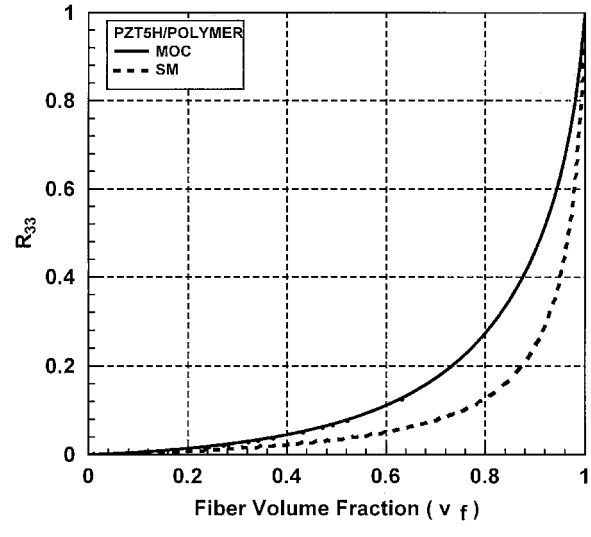

Fig. 9 Variation of the effective piezoelectric coefficient e_{33}^c of PZT5H/polymer composite with the fiber volume fraction.

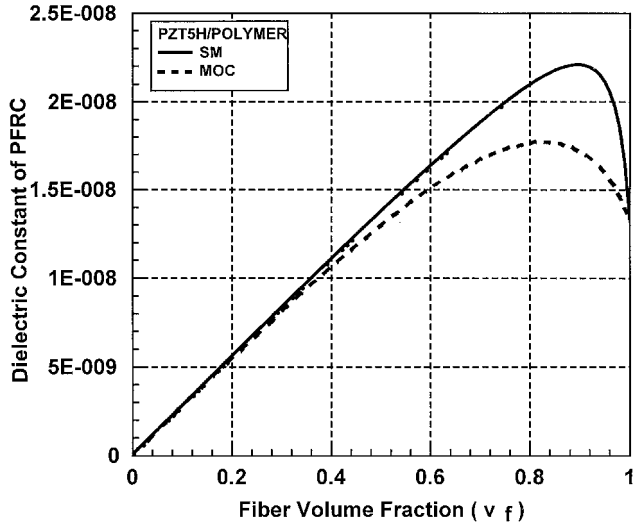

Fig. 10 Variation of the effective dielectric coefficient ε_{33}^{c} of PZT5H/polymer composite with the fiber volume fraction.

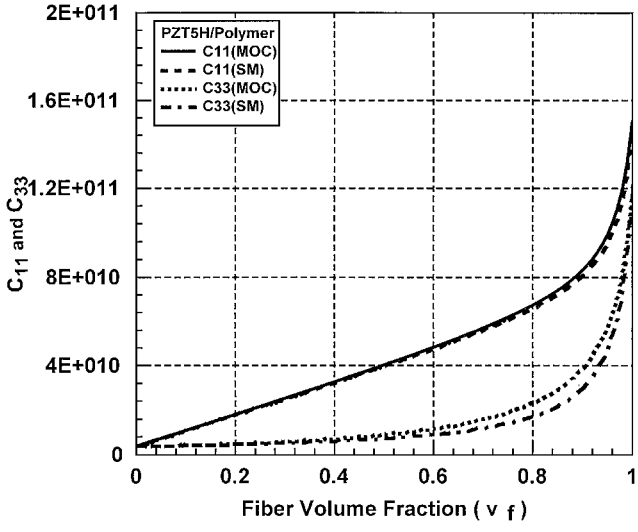

Fig. 11 Variation of the effective elastic coefficients C_{11}^{c} and C_{33}^{c} of PZT5H/polymer composite with the fiber volume fraction.

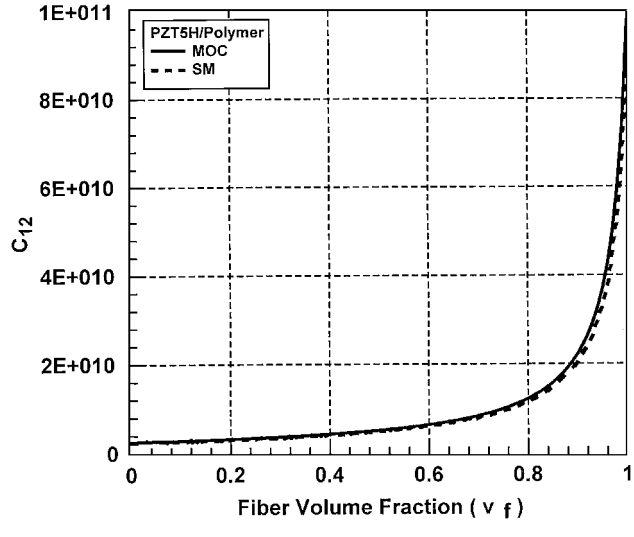

Fig. 12 Variation of the effective elastic coefficient C_{12}^{c} of PZT5H/polymer composite with the fiber volume fraction.

The variation of effective dielectric constant ε_{33}^{c} of the PFRC with the fiber volume fraction can be seen in Fig. 10 for PZT5H/polymer composite. Both methods are found to predict the same results in the practical range (<0.8) of interest for the fiber volume fraction. All of the effective elastic constants $\boldsymbol{C}_{ij}^{c}$ of the PFRC can be easily found once the matrix [**Z**] is evaluated for a particular fiber volume fraction. Figures 11 and 12 show the predictions of three such effective elastic constants of the PFRC. Note that the predictions by the two methods differ negligibly from each other. The similar predictions for the other effective elastic constants have also been obtained, but are not shown here.

Conclusions

In this paper, micromechanical analyses have been carried out to determine the effective coefficients of longitudinal PFRC. Two methods of micromechanics have been employed to compare the predictions. In the analyses, a constant electric field is considered to act only in the direction transverse to the fiber direction. The main objective of the work was to determine the effective piezoelectric constant $\boldsymbol{e}_{31}^{c}$ of the PFRC that determines the actuating force in the fiber direction due to the constant electric field transverse to the fiber direction. Predictions of this coefficient ($\boldsymbol{e}_{31}^{c}$) by both methods of micromechanics are in excellent agreement in the useful range of fiber volume fractions. For the materials of the piezoelectric fiber considered in this study, it has been found that, beyond a critical fiber volume fraction, this effective coefficient ($\boldsymbol{e}_{31}^{c}$) significantly improves over the corresponding coefficient of the piezoelectric material of the fiber. This indicates that the piezoelectric materials, superior to the existing monolithic one, can be tailored according to the design requirement. The predictions for the other effective piezoelectric constants, $\boldsymbol{e}_{32}^{c}$ and $\boldsymbol{e}_{33}^{c}$, which measure actuations in the directions transverse to the fiber, are also presented. The predictions of the effective elastic constants and the dielectric constant by both methods differ negligibly. Because the present methods produce almost identical predictions of the most important effective coefficients ($\boldsymbol{e}_{31}^{c}$, $\boldsymbol{C}_{11}^{c}$, and ε_{33}^{c}) of the proposed PFRC, which allow the PFRC to become distributed actuators for flexural vibration control, the present micromechanical models may be reliably used to predict the effective coefficients of PFRC. Although the experimental verification of the present work turns out to be beyond the scope of this paper, the present investigations may be a stride toward developing new, efficient smart materials and may serve as a reference for further work.

References

[1]Bailey, T., and Hubbard, J., "Distributed Piezoelectric-Polymer Active Vibration Control of a Cantilever Beam," *Journal of Guidance, Control, and Dynamics*, Vol. 8, No. 5, 1985, pp. 605–611.

[2]Crawley, E. F., and Luis, J. D., "Use of Piezoelectric Actuators as Elements of Intelligent Structures," *AIAA Journal*, Vol. 25, No. 10, 1987, pp. 1373–1385.

[3]Baz, A., and Poh, S., "Performance of an Active Control System with Piezoelectric Actuators," *Journal of Sound and Vibration*, Vol. 126, 1988, pp. 327–343.

[4]Tzou, H. S., and Tseng, C. I., "Distributed Piezoelectric Sensor/Actuator Design for Dynamic Measurement/Control of Distributed Parameter Systems," *Journal of Sound and Vibration*, Vol. 138, 1990, pp. 17–34.

[5]Lee, C. K., "Theory of Laminated Piezoelectric Plates for the Design of Distributed Sensors/Actuators. Part I: Governing Equations and Reciprocal Relationships," *Journal of the Acoustical Society of America*, Vol. 87, No. 3, 1990. pp. 1144–1158.

[6]Wang, B. T., and Rogers, C. A., "Laminate Plate Theory for Spatially Distributed Induced Strain Actuators," *Journal of Composite Materials*, Vol. 25, No. 4, 1991, pp. 433–452.

[7]Ha, S. K., Keilers, C., and Chang, F. K., "Finite Element Analysis of Composite Structures Containing Distributed Piezoceramic Sensors and Actuators," *AIAA Journal*, Vol. 30, No. 3, 1992, pp. 772–780.

[8]Hanagud, S., Obal, M. W., and Calise, A. J., "Optimal Vibration Control by the use of Piezoceramic Sensors and Actuators," *Journal of Guidance, Control, and Dynamics*, Vol. 15, No. 5, 1992, pp. 1199–1206.

[9]Rao, S. S., and Sunar, M., "Analysis of Distributed Thermopiezoelastic Sensors and Actuators in Advanced Intelligent Structures," *AIAA Journal*, Vol. 31, No. 10, 1993, pp. 1280–1286.

[10]Ray, M. C., Rao, K. M., and Samanta, B., "Exact Analysis of Coupled Electroelastic Behavior of a Piezoelectric Plate Under Cylindrical Bending," *Computers and Structures*, Vol. 45, 1992, pp. 667–677.

[11]Ray, M. C., Bhattacharyya, R., and Samanta, B., "Exact Solution for Static Analysis of Intelligent Structures," *AIAA Journal*, Vol. 31, No. 9, 1993, pp. 1684–1691.

[12]Ray, M. C., Bhattacharyya, R., and Samanta, B., "Finite Element Model for Active Control of Intelligent Structures," *AIAA Journal*, Vol. 34, No. 9, 1996, pp. 1885–1893.

[13]Han, J. H., and Lee, I., "Analysis of Composite Plates with Piezoelectric Actuators for Vibration Control Using Layerwise Displacement Theory," *Composites: Part B, Engineering*, Vol. 29, No. 5, 1998, pp. 621–632.

[14]Ray, M. C., "Optimal Control of Laminated Plate with Piezoelectric Sensor and Actuator Layers," *AIAA Journal*, Vol. 36, No. 12, 1998, pp. 2204–2208.

[15]Smittakorn, W., and Heyliger, P. R., "A Discrete-Layer Model of Laminated Hygrothermopiezoelectric Plates," *Mechanics of Composite Materials and Structures*, Vol. 7, No. 1, 2000, pp. 79–104.

[16]Oh, I., Han, J. H., and Lee, I., "Thermopiezoelastic Snapping of Piezolaminated Plates Using Layerwise Nonlinear Finite Elements," *AIAA Journal*, Vol. 39, No. 6, 2001, pp. 1188–1197.

[17]Sun, D., Tong, L., and Wang, D., "Vibration Control of Plates Using Discretely Distributed Piezoelectric Quasi-Modal Actuators/Sensors," *AIAA Journal*, Vol. 39, No. 9, 2001, pp. 1766–1772.

[18]Baz, A., "Active Constrained Layer Damping," U.S. Patent 5,485,053, 1996.

[19]Ray, M. C., and Baz, A., "Control of Non-Linear Vibration of Beams Using Active Constrained Layer Damping," *Journal of Vibration and Control*, Vol. 7, 2001, pp. 539–549.

[20]Ray, M. C., Oh, J., and Baz, A., "Active Constrained Layer Damping of Thin Cylindrical Shells," *Journal of Sound and Vibration*, Vol. 240, No. 5, 2001, pp. 921–935.

[21]Newnham, R. E., "Composite Piezoelectric Transducers," *Materials Engineering*, Vol. 2, 1980, pp. 93–106.

[22]Bennett, J., and Hayward, G., "Design of 1–3 Piezocomposite Hydrophones Using Finite Element Analysis," *IEEE Transactions on Ultrasonics, Ferroelectrics and Frequency Control*, Vol. 44, 1997, pp. 565–574.

[23]Sigmund, O., Torquato, S., and Aksay, I. A., "On the Design of 1–3 Piezocomposite Using Topology Optimization," *Journal of Material Research*, Vol. 13, 1998, pp. 1038–1048.

[24]Smith, W. A., and Auld, B. A., "Modeling 1–3 Composite Piezoelctrics: Thickness Mode Oscillations," *IEEE Transactions on Ultrasonics, Ferroelectrics, and Frequency Control*, Vol. 40, 1991, pp. 40–47.

[25]Dunn, M. L., and Taya, M., "Micromechanics Predictions of the Effective Electroelastic Modulii of Piezoelectric Composites," *International Journal of Solids and Structures*, Vol. 30, 1993, pp. 161–175.

[26]Aboudi, J., "Micromechanical Prediction of the Effective Coefficients of Thermo-Piezoelectric Multiphase Composites," *Journal of Intelligent Material Systems and Structures*, Vol. 9, 1998, pp. 713–722.

[27]Cady, W. G., *Piezoelectricity*, McGraw–Hill, New York, 1946.

M. Ahmadian
Associate Editor